

# NUMERICAL STUDY OF COHERENT HARMONIC GENERATION IN THE VUV ON THE NIJI-IV FEL

H.Ogawa<sup>#</sup>, K. Yamada, N. Sei, M. Yasumoto, T. Mikado,

National Institute of Advanced Industrial Science and Technology, 1-1-1 Umezono, Tsukuba,  
Ibaraki 305-8568, Japan

**Abstract**

Generation of the VUV radiation has been numerically performed based on coherent harmonic generation (CHG) scheme at NIJI-IV with an external laser. The CHG process in an optical klystron was simulated using the code GENESIS1.3 incorporating with its extended code. After performing the optimization of the parameter for the optical klystron, the dependence of the input laser power and the effect of the energy spread on the output radiation power are discussed.

## INTRODUCTION

Coherent harmonic generation (CHG) is an attractive method as a source of tunable coherent radiation in the VUV. Considering advantage of operation without an optical cavity in CHG, we are preparing to produce the harmonics in the storage ring NIJI-IV FEL [1] by using either an external laser focused into an optical klystron [2,3] or the FEL oscillator itself. In this study we focus on the investigation of the harmonic generation by an external laser (3rd harmonic of Nd:YAG laser) with Monte Carlo simulation.

The layout of the CHG in the transverse optical klystron, which consists of three sections, is illustrated in Fig. 1. In the first section, the energy exchange between the electron beam and the optical wave, supplied by an external pulsed laser, induces the energy modulation of the electron. In the second section, the energy modulation is transformed into an electron density modulation. The amplitude of the magnetic field in the dispersive section is optimized so as to obtain the maximum radiation intensity at the end of the optical klystron. Consequently, in the last section, the coherent harmonic radiation is emitted from the second undulator. In this work, this CHG process is

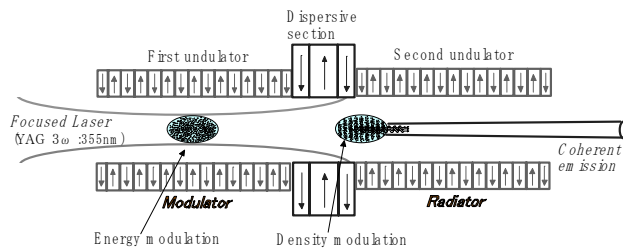


Figure 1: Schematic view of the setup for Coherent Harmonic Generation (CHG).

simulated in the case of a 6.3-m optical klystron ETLOK-II [1].

## PROCEDURE OF SIMULATION

The electron beam is interacted with the third harmonic at 355nm of an external Nd:YAG laser which is focused into the center of the first undulator as shown in Fig.1. The electron beam dynamics in the first undulator is simulated along the undulator axis by using the code GENESIS 1.3 [4] which allows for the treatment of three-dimensional electron dynamics and non-axi-symmetric radiation field. The initial parameters for the electron beam at the entrance of the optical klystron are listed in Table 1. The external laser beam field is taken to be a fundamental Hermite-Gauss mode, and the magnetic field parameter of the undulator is chosen so that the wavelength of the external laser is resonated with the fundamental radiation of the undulator. As a result, the 6D phase space distribution  $(x,y,p_x,p_y,\gamma,\theta)$  of the electron beam at the exit of the first undulator is obtained by GENESIS 1.3.

Table 1: Simulation parameters for the NIJI-IV FEL system.

<i>Electron beam</i>	
Energy	310 MeV
Relative energy spread	$3.3 \times 10^{-4}$
Bunch length	17.4mm
Beam size $\sigma_x$	$\sim 0.8$ mm
$\sigma_y$	$\sim 0.3$ mm
Emittance $\epsilon_x$	$6.0 \times 10^{-8}$ m rad
$\epsilon_y$	$8.4 \times 10^{-9}$ m rad
<i>Optical Klystron</i>	
Magnetic period	
Undulator section	72mm
Dispersive section	216mm
Number of period	42×2
Total length	6.288m
K-value	2.29
<i>Input laser (Nd:YAG)</i>	
Wavelength	355nm
Energy	300mJ/pulse
Peak power	60MW
Repetition rate	10Hz

<sup>#</sup>ogawa.h@aist.go.jp

In the dispersive section, the phase shift is induced by the different transit time depending on the difference of the electron energy. We took the phase energy relation [5]

$$\Psi_j = \frac{\omega_{s1}}{\omega_{s2}} \left[ \theta_j + \frac{d\theta}{d\gamma} (\gamma_j - \gamma_0) \right] \quad (1)$$

between the ponderomotive phase of the electron  $\theta_j$  and  $\Psi_j$  at the entrance and the end of the dispersive section for  $j$ th electron, respectively. Here  $\gamma_j - \gamma_0$  is the energy deviation from the mean energy of the electron beam in terms of the Lorentz factor, and the ratio  $\omega_{s1}/\omega_{s2}$  gives the harmonic number of the input laser. The factor  $d\theta/d\gamma$  is a function of length and field strength of the dispersive section. Inserting the phase distribution at the end of the first undulator calculated by GENESIS 1.3 into Eq.(1), the 6D phase space distribution  $(x, y, p_x, p_y, \gamma, \Psi)$  at the exit of dispersive section is determined.

Thus, the obtained parameters  $x, y, p_x, p_y, \gamma, \Psi$  are written into a file as an input to GENESIS 1.3 for calculation in the second undulator. The coherent emission from the bunched electrons is again simulated along the second undulator axis using GENESIS 1.3, and then we get the harmonic radiation distribution at the exit of the optical klystron.

## SIMULATION RESULTS

### Optimization of the optical beam waist

First of all, the dependence of the third harmonic intensity on the radius of the optical beam waist  $w_0$  was investigated. The number of emitted photons corresponding to the three different input laser powers  $P_{in}=30, 60$  and  $90$  MW is plotted in Fig.2. In this simulation, the factor  $d\theta/d\gamma$  in Eq.(1) was chosen so as to obtain the maximum harmonic intensity for the corresponding  $P_{in}$  and harmonic number. For example  $d\theta/d\gamma=0.3$  is the optimum value for the third harmonic at  $P_{in}=60$  MW.

As shown in Fig.2, the output intensities grow with increasing the waist size  $w_0$  up to  $w_0 \sim 1.0$  mm since the overlap of the electron beam with the optical wave increases. On the other hand, above  $w_0 \sim 1.4$  mm, the intensities decrease due to diminishing electric field of pumping laser. It is interesting to note that the waist size  $w_0$ , which gives the maximum harmonic intensity, increases with increasing  $P_{in}$ . This optimum  $w_0$  shift can be understood as the inhomogeneous transverse profile of electron bunching. For the low  $P_{in}$ , electric field of laser is insufficient to produce the electron density modulation, so the waist size  $w_0$  must be reduced. On the contrary, for the high  $P_{in}$ , overbunching of the electron density occurs in the center of the beam, thus reducing the efficiency of the harmonic generation. To avoid the overbunching, the  $w_0$  should be larger value, giving constant radial profile of the electron bunching.

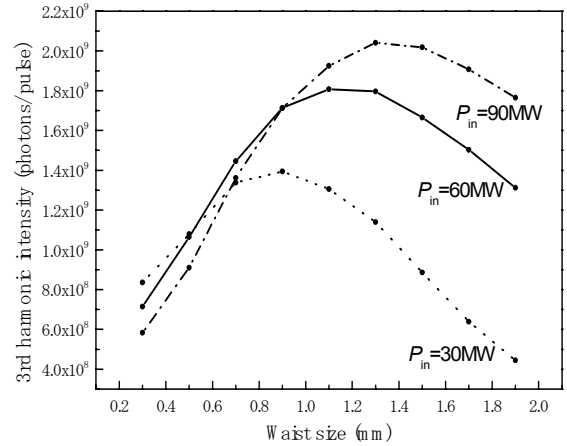


Figure 2: Dependence of the third harmonic intensity on the radius of the optical beam waist at the input laser power  $P_{in}=30, 60$  and  $90$  MW with the electron average current  $1$  mA.

### Power Dependence

Figure 3 shows the calculated photon intensities on the third and fifth harmonics of a pumped laser at  $355$  nm as a function of the laser peak power  $P_{in}$ . The calculation has been also performed taking into account an optimization of  $d\theta/d\gamma$  parameter for each  $P_{in}$ , while  $w_0$  is fixed at  $1.1$  mm. The number of photons increases proportional to  $P_{in}$  in low laser power region, and is saturated above  $\sim 60$  MW owing to the overbunching effect, giving a limit of the harmonic intensity. In the case of our laser power,  $P_{in} = 60$  MW, the number of photons were calculated as  $\sim 2 \times 10^9$  and  $\sim 3 \times 10^8$  photons/pulse for the third and fifth harmonics, respectively, at the electron average current  $1$  mA in one bunch ring operation.

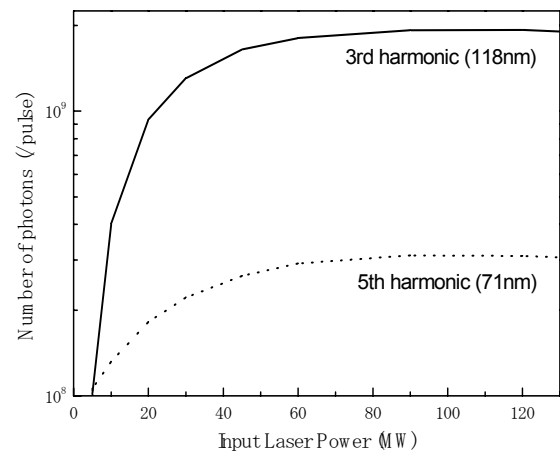


Figure 3: Calculation results of number of photons on the third and fifth harmonics as a function of the input laser power with the electron average current  $1$  mA.

### Effects of the Energy Spread

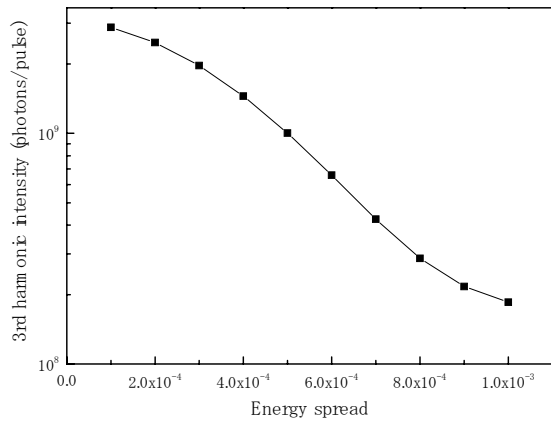


Figure 4: Effects of the relative energy spread on the output intensity.

Figure 4 shows the calculation result of dependence of the third harmonic intensity on the relative energy spread at the entrance of the first undulator. The efficiency of harmonic generation is critically dependent on the energy spread value.

The phenomenon which increases the energy spread, called turbulent anomalous bunch lengthening, appears above a certain current threshold. The anomalous bunch lengthening has been observed in NIJI-IV above an average current of 2-3 mA [6,7]. The obtained third harmonic intensity, which was simulated taking into account the effect of increasing energy spread with the beam current, is shown in Fig.5 by dash-dotted line. The photon intensity is saturated at  $\sim 5 \times 10^{10}$  photons/pulse due to the energy spread at higher beam current beyond the threshold current.

Recently we have replaced ring vacuum chambers in NIJI-IV with new low-impedance-type ones over 75 % of the ring circumference in order to suppress the microwave instability. [7]. After the replacement, the longitudinal broad-band impedance was reduced and the anomalous bunch lengthening doesn't appear below 15.3 mA which means energy spread of the beam is stable below  $\sim 15$  mA in the present experimental setup. As shown in Fig.5 by solid line, the third harmonic intensity grows proportional to the square of the average beam current in one bunch ring operation. Consequently, the number of photons on

the third harmonic can be expected to obtain  $\sim 4 \times 10^{11}$  photons/pulse and increase by a factor of 8 for the new vacuum-chamber system compared to the old one.

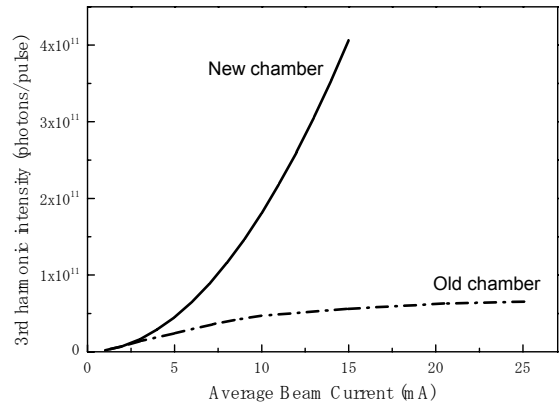


Figure 5: Expected number of photons for the new and old vacuum-chamber system as a function of the average beam current in one bunch ring operation.

### ACKNOWLEDGMENTS

The authors would like to thank Dr. H. Xu for useful discussion. This study was financially supported by the Budget for Nuclear Research of the Ministry of Education, Culture, Sports, Science and Technology, based on the screening and counseling by the Atomic Energy Commission.

### REFERENCES

- [1] T. Yamazaki *et al.*, Nucl. Instr. and Meth. A331 (1993) 27.
- [2] K. Yamada *et al.*, Nucl. Instr. and Meth. A407 (1998) 193.
- [3] H. Xu *et al.*, Proc. of PAC01, Chicago, 2001, p.2836.
- [4] S. Reiche, Nucl. Instr. and Meth. A429 (1999) 243.
- [5] L.H. Yu, Phys. Rev. A44 (1991) 44.
- [6] K. Yamada *et al.*, Nucl. Instr. and Meth. A475 (2001) 205.
- [7] K. Yamada *et al.*, Proc. 24<sup>th</sup> Free Electron Lasers Conf., Argonne, 2002, to be published